Hittite Journal of Science and Engineering, 2018, 5 (1) 37-48
ISSN NUMBER: 2148-4171
DOI: 10.17350/HJSE19030000076

Rehabilitation of Francis Turbines of Power Plants with Computational Methods

Kutay Celebioglu[1] Selin Aradag[1,2] Ece Ayli[1,3] and Burak Altintas[1,2]
[1] TOBB University of Economics and Technology, Hydro Energy Research Laboratory, Ankara, TURKEY
[2] TOBB University of Economics and Technology, Department of Mechanical Engineering, Ankara, TURKEY
[3] Cankaya University, Department of Mechanical Engineering, Ankara, TURKEY

ABSTRACT

Rehabilitation of existing hydroelectric power plants (HEPP) by redesigning the hydraulic turbines is usually more elaborate than designing a tailor-made turbine for a new plant. Some of the parts are buried and the space is limited with the size of the old turbine; therefore, this increases the number of constraints imposed on the design. This article presents a Computational Fluid Dynamics (CFD) based rehabilitation procedure involving the state of the art redesign of the turbine of a hydroelectric power plant for better performance at design and off-design conditions of several head and flow rates. Runner and guide vanes of the Francis turbine are designed per the design head and flow rates available for the turbine at the site. The simulations for the designed parts are performed both separately and using all turbine parts as full turbine analyses. Both the design and off-design conditions are simulated for the newly designed and existing turbines for comparison purposes. Cavitation performance of the new design is also determined. The proposed methodology is applicable to any Francis type turbine and any HEPP that needs rehabilitation.

Article History:
Received: 2017/05/08
Accepted: 2017/11/14
Online: 2018/03/28

***Correspondence to**: Kutay Celebioglu, TOBB University of Economics and Technology, Hydro Energy Research Laboratory (ETU Hydro), Ankara, TURKEY*
Tel: +90 (312) 292-4473
E-Mail: tkcelebioglu@etu.edu.tr

Keywords:
Francis turbine; Rehabilitation; Efficiency; Runner; Guide vane

INTRODUCTION

Rehabilitation of hydraulic turbines of existing power plants is an important topic because of the low performance, poor reliability, frequent maintenance intervals and undesirable cavitation properties of old turbines at the plants. Rehabilitation projects increased worldwide to improve turbine designs and to reach the desired performance characteristics, especially with the improvements in computational power and Computational Fluid Dynamics (CFD) technology. However, rehabilitation of old power plants is often more difficult than the design of the turbines for new power plants since most of the existing parts cannot be altered because some of the parts are buried and the space is limited with the size of the old turbine.

Both experimental and numerical methods are common in the design [1] and rehabilitation of Francis turbines. Performing numerical simulations is an efficient approach as an alternative to model tests. Steady state and transient Francis turbine simulation results are presented in the study of Beatove et al. [2]. Interactions between turbine components (such as rotor and stator) are investigated and fluctuating pressure dynamics are obtained with transient simulations. Experimental measurements are also performed using dynamic pressure sensors and strain gages. Numerical results agree well with the experiments. Qian et al. [3] worked on three-dimensional, unsteady, multiphase flow simulations for the whole Francis turbine. Numerical analysis is performed with a commercial CFD software and sliding mesh model is used to obtain time dependent results. Pressure pulsations are analyzed via Fast Fourier Transform (FFT). Their experimental and numerical results agree well. Su et al. [4] computed the three-dimensional turbulent flow in Francis turbines using Large Eddy Simulations (LES). They used unstructured meshes for the spiral case and the runner, while structured meshes were utilized for the remaining components. They found out that cavitation was observed at the suction side of the blade under partial load conditions. Patel et al. [5] also performed three-dimensional, unsteady CFD simulations for Francis turbines. They investigated the effect of partial loading on turbine performance. The

efficiency first increases up to full operating load and then it starts to decrease. Head loss variations are investigated in detail by using velocity plots. Turbine performance is predicted both at the best efficiency point and at partial load conditions which shows improvement over the existing design. Kaniecki et al. [6] re-engineered the runner and guide vanes of the Grodek and Kamienna hydroelectric power plants. The efficiency of Kamienna HEPP increased from 75% to 85%. Akin et al. [7] developed a design methodology for Francis turbines. Overall turbine efficiency can reach up to 92.3% with their design methodology. Gohil and Sanini [8] considered a Francis turbine with a capacity of 225 kW power in their simulations. CFD results agree with model tests. Shukla et al. [9] aimed to validate their three dimensional CFD results with experimental findings, as well.

There are several rehabilitation studies worldwide; however, the results are usually neither generalized nor published in archival publications. Bornard et al [10] report the results of several rehabilitation projects. Xi-de and Yuan [11]. In some of these projects, the guide vanes and the runner are the only modified parts as in this study. However, in some of them, rehabilitation of other components were also found feasible and performed. In two of the projects reported by Bornard et al. [10] stay vanes are modified and efficiency gains of less than 1% are obtained. However, when the guide vanes and runners are altered, the efficiency gains are more than 3% as in Chute des Passes, Shasta and Yinxiuwan projects explained in detail by Bornard et al. [10], Michel and Kunz [12] and Xi-de & Yuan [11]. Cavitation characteristics can also be improved when the runner is modified as in Kelsey project, reported by Bornard et al. [10].

Kepez 1 hydroelectrical power plant, located in Antalya, Turkey, was constructed in 1960's. It has three identical Francis type turbines. Redesign of the turbine is performed based on CFD. The design criteria are higher efficiency, power output, no cavitation and wider operating range. The plant has been utilized for several years and accumulation of lime on pipe surfaces is unavoidable because of the water characteristics in the area. How lime accumulation affects the friction factor is an important concern because the losses in the pipe can alter the head and flow rate specifications of the turbine to be designed, drastically. Therefore, the friction factor of the pipes and equipment of the plant is determined through experimental measurements at the site and analysis of the whole pipe and power system as a network. The new turbine is designed per the design head and flow rates determined based on this experimentally obtained friction factor. Off-design performance of the runner is also tested using several possible operating points.

The scope of this work includes redesign of the guide vanes and runner using available data for other turbine parts and on-site measurement of the geometries. The simulations for the designed parts are performed both separately and using all turbine parts as full turbine analyses. Both the design and off-design conditions are simulated for the designed and existing turbines for comparison purposes. Cavitation performance of the new design is also determined. The proposed methodology is applicable to any Francis type turbine and any HEPP that needs rehabilitation.

METHODOLOGY

The first step in the turbine rehabilitation process is to decide on the head and flow rate values of the power plant. The friction factor was found to be 0.014 for the pipes based on experimental measurements of pressure values and system analysis using Watercad, which is a commercial software to perform network analysis of pipe systems [13]. The friction factor is utilized to obtain head losses, then to determine the available head for the turbine. The whole CFD study is based on this head value. The expected performance values of the plant, based on the hydraulic analysis of the system are summarized in

Table 1 General performance values for the HEPP.

Head (m)	*162*
Power (MW)	*8.8 MW/turbine*
Rotational Speed (rpm)	*750*
Flowrate (m^3/s)	*6.1*
Turbine efficiency	*92%*

The existing turbines cannot produce the expected power. Vibration and noise occur at partial load conditions, as well. Erosion and damage are also observed at the trailing edge of the guide vane and at the suction side of the runner as shown in Fig. 1, most probably due to cavitation.

Original guide vanes and runner are redesigned. Other parts are buried to concrete, they cannot be changed; however, they play an important role in full turbine CFD simulations. The design procedure starts with the CFD part for rehabilitation since the geometry is restricted with the

Figure 1. Picture of the existing guide vane and the runner

parts that are buried. Critical parameters for the guide vane and runner, blade angle distribution, blade thickness, inlet and outlet diameter are optimized to reach higher efficiencies with no cavitation. Fig. 2 shows the flow chart of the entire design process. First step is the preparation of the geometry for simulations. CAD models of the replaceable turbine parts are obtained through laser scanning of the actual parts at the site. Measured geometries are compared with the available technical drawings. The technical drawings of the buried parts, which are the spiral case, stay vane and draft tube of the turbine, are used in the CFD analysis. CAD model of the existing turbine is shown in Fig.3.

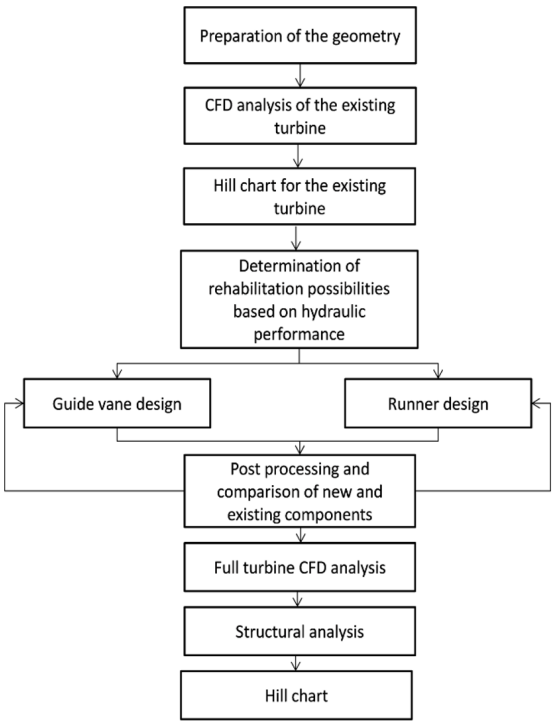

Figure 2. Design flow chart

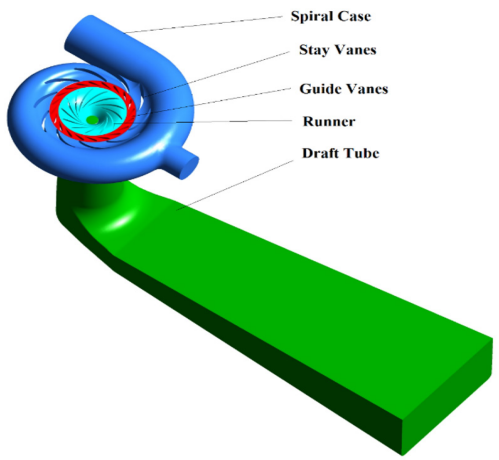

Figure 3. CAD model of the existing turbine

After conducting separate CFD analysis of the components, full turbine analyses for nominal and partial loads are performed to obtain a hill chart that shows the performance of the turbine. The analyses at off-design points help to examine the performance of the turbine at partial load conditions, as well. The problems of the existing turbine are examined through turbine efficiency curves, flow angles and pressure distributions. The guide vanes and runner are redesigned to ensure better cavitation characteristics and hydraulic performance for both nominal and partial loads. The hill chart for the newly designed turbine is also constituted.

ANSYS CFX [14] software is utilized. Finite Volume Method that solves the incompressible pressure-based Reynolds Averaged Navier-Stokes (RANS) equations is employed. k- ε turbulence model is used. High order upwind and second order centered schemes are used for the convection and diffusion terms, respectively.

Cavitation simulations are implemented with homogeneous multiphase model which allows modeling the mixture as a pseudo-fluid. Thus, the governing equations consist of mass conservation, a set of momentum equations and a transport equation for the volume fraction. Shear Stress Transport (SST) is used as turbulence model to solve Reynolds Averaged Navier-Stokes (RANS) equations, which combines k-ω and k-ε turbulence models. It resolves flow separations accurately near the walls. Rayleigh Plesset model is implemented for the detection of cavitation. Steady-state cavitation simulations are performed using the solution of the corresponding steady-state simulations without cavitation as an initial condition. The convergence level is set to $1x10^{-5}$.

Multi frame reference model (MFR) is used to model the interaction of the parts with each other [15]. Runner is attached to the guide vane and draft tube by frozen rotor interface. There are several recent studies in literature in which the interactions between runner-guide vane and runner-draft tube are included via frozen rotor interface. For example, Lenarcic et al. [16] simulated incompressible turbulent flow for a high head Francis turbine under steady operating conditions which is computed using an open source code. Influences of the coupling methods are compared with each other and with experimental data. Frozen rotor coupling method results are compatible with the experimental results. Tonello et al [17] worked on steady-state operation of Francis-99, Tokke turbine at different loads. Simulations are carried out using both the frozen rotor approximation and unsteady sliding mesh technique. It is found out that sliding mesh approach does not offer significant advantage when compared to the frozen rotor model based on comparisons with each other and experimental

Table 2. Mesh properties for runner.

Mesh quality	Number of nodes	Number of elements	Min y+	Number of elements in the boundary layer
Low	240771	221100	100	10
Medium	417911	388320	50	10
High	708700	664950	25	10
Very high	917472	865050	10	10

data. Laouari and Ghenaiet [18] used frozen rotor interface to simulate the turbulent flow through a small horizontal Francis turbine. Hydraulic performance is presented for different rotational speeds. Predicted performance shows that at the nominal point, maximum hydraulic efficiency reaches 79.28% and there is an important drop with increased discharge.

Pressure inlet, mass flow outlet boundary conditions are used for the design of the runner and guide vanes. For full turbine analyses, which comprise the simulations of all turbine components, mass flow inlet and pressure outlet are utilized as boundary conditions. All other parts are considered as no slip wall condition with a smooth wall assumption. In the design phase, it is found sufficient to model only one guide vane and runner and to use circumferential averaging, therefore periodic interfaces. However, for full turbine analyses, whole system containing the guide vanes, stay vanes and runner blades are used to observe the general performance of the system.

Computational domain for the design of the runner is only the runner itself. Therefore, CFD analyses are performed using HP Z840 workstations, which have Intel(R) Xeon(R) CPU E5-2640 v3 2.60GHz 16 (32 cores) and 64.0 GB installed RAM. One solution takes approximately 30 minutes using this computer. When the runner design is finished, full turbine analyses, the computational domain of which is composed of the spiral case, stay vanes, guide vanes, runner and draft tube, are performed by using a supercomputer clustered from 11 nodes HP Proliant DL380p Gen8, which have Intel(R) Xeon(R) E5-2695v2 2.40 GHz Turbo 3.2GHz (12 Cores) and 64.0 GB installed memory (RAM) in each node. A solution for head and flow rate combination takes 7-8 hours using this supercomputer facility with 120 processors.

Mesh independency study is performed separately for all components. As runner is the major component of the turbine, it is crucial to check the mesh independency of the solution to have accurate runner parameters such as runner hydraulic efficiency and power. Mesh properties for the runner are given in Table 2, as a representation of the mesh independency study performed.

The result of mesh independency study for runner in terms of output parameters is given in Table 3. High quality meshes are used for further runner computations based on the results of the grid refinement study.

Summary of mesh independency study is given in Table 4. For single turbine analysis that comprises five components, 36x106 mesh elements are used. Separate meshes are used for rotating and stationary components due to the complexity of the geometries. Using same number of elements, cell size and distribution for all simulations is very difficult; therefore, Generalized Grid Interface (GGI) method is used to transfer all flow gradients through non-conformal meshes [19].

Table 4. Summary of the mesh independency study.

Component	Number of Elements
Spiral Case & Stay Vane	20,193,590
Guide Vane	222,690 x 20 = 4,453,800
Runner	664,950 x 13 = 8,644,350
Draft Tube	3,068,834
Total number of element	36,360,574

RESULTS AND DISCUSSION

Analysis of the existing turbine

Different opening percentages and different volumetric flow rates for each opening of guide vanes are necessary to develop a numerical hill chart for constant rotational speed. Analyses are performed for a range of head values (from 142 m to 173 m). For all head values, CFD analyses are performed for an operating range of %20 to %130 loading which is accomplished by adjusting the guide vane angles.

Table 3. Mesh independency study result for runner.

Control parameters	Low Quality Mesh	Medium Quality Mesh	Relative Error (%)	High Quality Mesh	Relative Error (%)	Very High Quality Mesh	Relative Error (%)
ΔH	0.909	0.905	0.442	0.905	0.033	0.905	0.011
Head (m)	157.987	156.412	1.007	155.170	0.800	155.620	0.289
Efficiency (%)	96.915	97.195	0.288	97.322	0.130	97.367	0.046

Head-discharge operating characteristics of the existing turbine are shown in Fig. 4. The graph shows the isoclines of the efficiency (η). 52 full turbine simulations for different guide vane openings and head values, with 36 million grid points each, are simulated to obtain hill chart that demonstrates the behavior of the turbine for a wide range of head and flow rates representing the off-design conditions of turbine operation. The area between the black lines, denote the turbine operating range. In an efficient design, design point should be in the middle of the hill chart and the operating range with maximum efficiency value. On the other hand, in the existing design, the design point cannot reach the maximum efficiency of the system, and the operating region is not settled at the high efficiency zone. When the turbine is used off limits, keeping the efficiency as high as possible is an important constraint. Therefore, in the new design, the operating range should be widened and must be inside the maximum efficiency region.

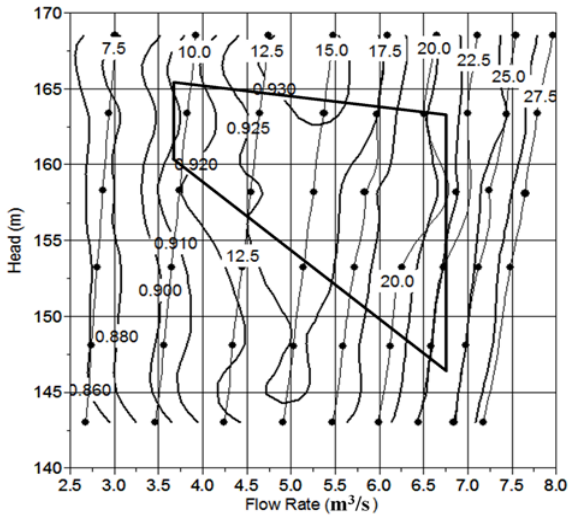

Figure 4. Hill chart for the existing turbine.

Hydraulic energy is converted to mechanical energy by decreasing the pressure significantly inside the runner. Pressure can be below the vapor pressure which induces cavitation at high loads. This is a very aggressive process which can cause material damage and performance drop in the overall turbine efficiency. To investigate cavitation in the turbine, pressures are examined. Cavitation occurs when the pressure is less than the vapor pressure (Pv) determined by site conditions as 4.24 kPa. In Fig. 5, pressure distribution on the existing runner blade at the design conditions is shown. It is seen that the pressures are below vapor pressure near the shroud, which causes cavitation.

To minimize this low-pressure zone, introducing a leaning from the shroud in the direction of rotation can be a solution [20]. Fig. 6 shows the meridoinal view of the turbine blades. Hub and shroud, as well as the leading and trailing edges of the runner are shown in the figure. The important

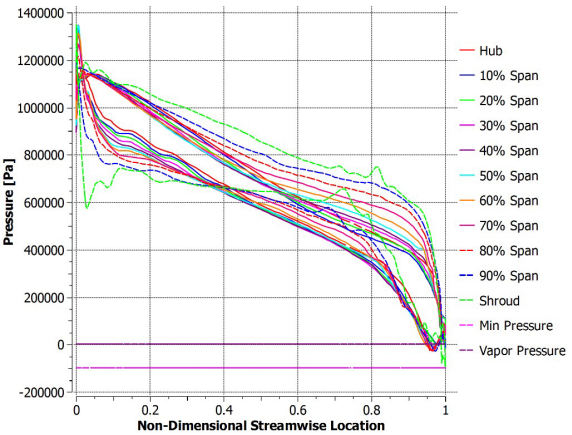

Figure 5. Pressure distribution on the existing runner blade at the design condition.

angles that define the runner geometry are shown in Fig. 7. Here, $\beta 1$ (for inlet) and $\beta 2$ (for outlet) are known as "Beta angles of the runner blade" or "the metal angles of the blade" [20]. In the same figure V_{1u} and V_{2u} are the circumferential velocities. w_2 is the relative speed at the outlet of the runner.

Velocity streamlines around the runner blades are shown in Fig 8. Vortices and seperation are observed at the pressure side of the runner blade. These cause performance

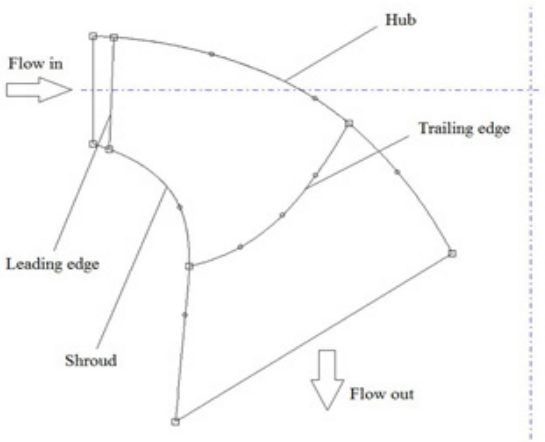

Figure 6. Meridional view of the runner.

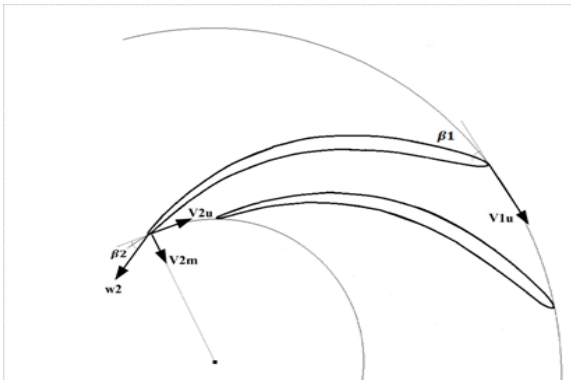

Figure 7. Axial view of the turbine runner blades.

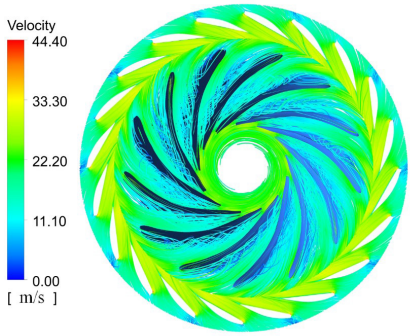

Figure 8. Velocity streamlines for full loading operation of the existing turbine (Head=162 m, 17.5° guide vane opening, 63.6% of full opening).

reduction in the runner. These formations are also one of the reasons of cavitation. Uniform flow distribution around the blade should be provided for the design conditions for rehabilitation of the turbine.

CFD based design of the new turbine

NACA 0016 profile is used for the final guide vane design (Fig. 9). Numerical weighted average efficiency increase is about 2.2 % for NACA0016 geometry at a net head of 157 m (Fig. 10). As seen in Fig. 10, when NACA 0018 profile is used for the guide vanes, the efficiency gain is not as high as the gain obtained with NACA 0016 profile. One important reason of this efficiency rise is the fact that the old guide vane is much rougher than the new one. The roughness is because of being in usage for several years and material erosion.

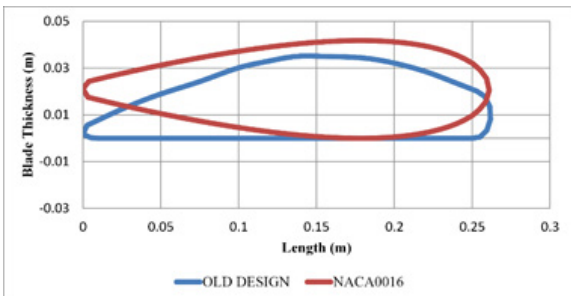

Figure 9. New and existing design geometries for the guide vanes.

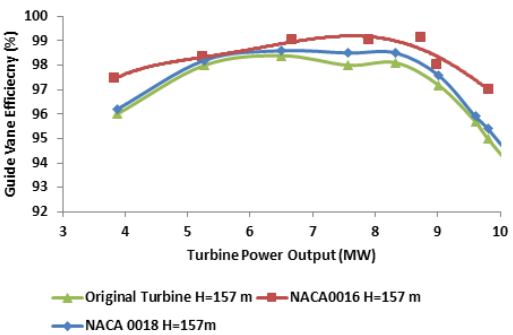

Figure 10. Guide vane efficiency versus turbine power output for the existing and new guide vanes.

The angle of guide vanes and their profile should be reasonably designed to achieve flow stability with no separation and vortices and maximum efficiency for design conditions. For some of the simulated guide vane opening angle alternatives, runner pressure distribution is shown in Fig. 11. For 20° and 17.5° guide vane openings, water hits to the suction side of the blade. Whereas, when the guide vane opening is changed to 15°, the flow hits to the leading edge of the runner blade.

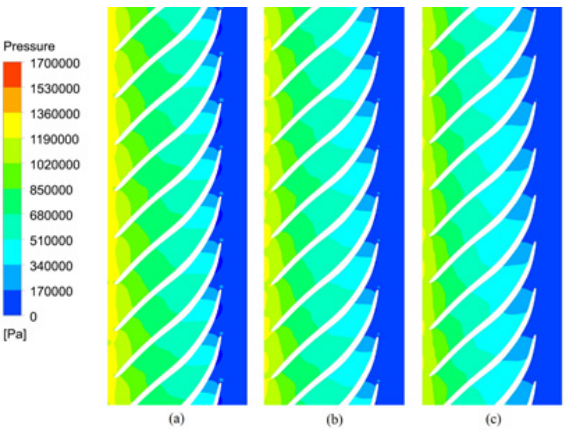

Figure 11. Runner pressure distribution for (a) 20° (b) 17.5° (c) 15° guide vane opening angles.

The angles of the runner blades, flow angles, blade length and thickness are important for runner design process. Several simulations are performed by changing these parameters. The required head, flow rate, power with maximum efficiency are obtained by making improvements in the design. In Table 5, all design cases are tabulated. Some of the designs are analyzed and compared with each other to observe the effect of each parameter on runner performance and cavitation characteristics.

The aim is to attain the required head and power values with high runner efficiency and better cavitation characteristics. The parameters that are optimized in the design are blade inlet and outlet edge slopes, beta and theta angle distribution for each layer of the blade and blade thickness profile. Blade profile lengths are increased near the hub layer by using beta angle distribution to improve the cavitation characteristics. In addition, guide vane angle is one of the most important parameters that control the uniform flow distribution through the leading edge to the trailing edge of the blade and it is modified, as well. It is kept around 16° for smooth velocity distribution and cavitation free performance.

Smooth beta distribution for the runner, which provides higher head and flow rate, is important. Leaning is provided from the leading edge of the runner from 1° to 5° to obtain balanced pressure distribution which is very important when using X-blade design. Leading edge beta value

is adjusted to make sure that leading edge separation disappears, however leading edge cavitation becomes the limit in the process of increasing leading edge beta angles. Trailing edge beta angles are changed between 11^0 and 19^0. This improves cavitation characteristics but the power can decrease if the angle becomes higher.

Shorter blade lengths and thick edges for the leading and trailing edges can decrease friction losses which increases efficiency. However, shorter blade lengths can make the blades prone to cavitation. Therefore, the blade length is only decreased twice in 2 cm increments. Beta angles for the hub and shroud are important for power increase and they are increased from 3^0 to 7^0. Theta distribution must be as linear as possible for cavitation; therefore, this fact is also kept in mind during the design process.

In Fig. 12, meridional profiles, which demonstrate full pattern of water flow in the runner, for the existing and new runners are shown. Blade length is gradually shortened. This decreases the friction losses on the blade and increases the efficiency for higher flow rates. However, shorter blade promotes cavitation.

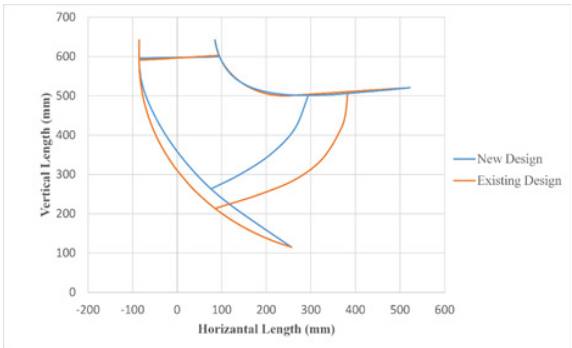

Figure 12. Meridional profile of the existing and new runners.

In Fig. 13, runner blade thickness change is shown. The original thickness distribution was changed to a NACA-profile (V18). The final runner blade is thicker than the existing runner which can also increase the mechanical strength of the runner. On the other hand, due to the contraction of the flow field, the possibility of exposure to cavitation increases. Leaning is defined from the hub to decease cavitation. Per previous studies of Ayli et al. [20, 21] and the results examined in this research, (V20 to V23), it is observed that increasing the lean in the direction of rotation improves the cavitation characteristics.

Conventional Francis turbine runners like the one under investigation in this research, are prone to cavitation damage on the suction side of the blade, especially to leading edge cavitation. Leading edge cavitation is one of the most hazardous types for Francis turbines. As it occurs at the inlet of the runner, damage is heavy; it causes vibration and provokes pressure fluctuations [22]. X-blade technology is

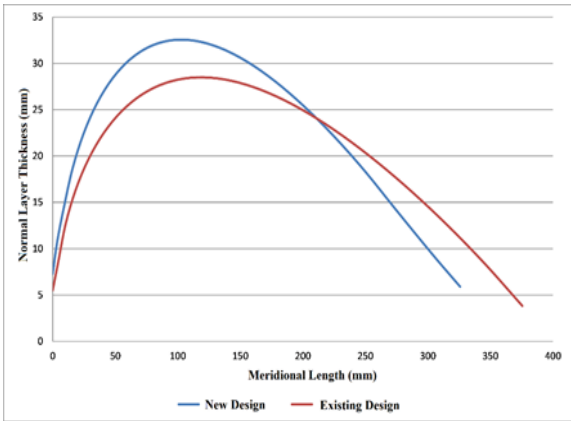

Figure 13. Runner thickness for the existing and new runner.

improved by Billdall and Holt [23] to eliminate leading edge cavitation and to increase the performance of the runner during the development of the Three Gorges Project in China. A pressure balanced design must be performed when using X-blade shapes. If the design is not pressure balanced, the dynamic loads which are larger at part-load conditions, increase the risk of blade cracking [24]. Although the manufacturing of X-blades is more difficult and costly and pressure balanced blade design is crucial, X-blade technology has been popular in the 2000's because of its advantages.

One series of runner blade versions comprise modifications that focus on improving the V_u distribution at the outlet of the blade [25]. The modifications are mainly focused on the trailing edge of the blade. In Fig.14, circumferential distribution of V_u for the existing and new runners is shown. Here, x-axis denotes the dimensionless spanwise location on the blade. 0 and 1 correspond to hub and shroud. Defining leaning from the hub inhibits the separations and low pressure zones in the flow which contribute to more energy release in the runner. As the result of this series of arrangements, circumferential velocity becomes more uniform.

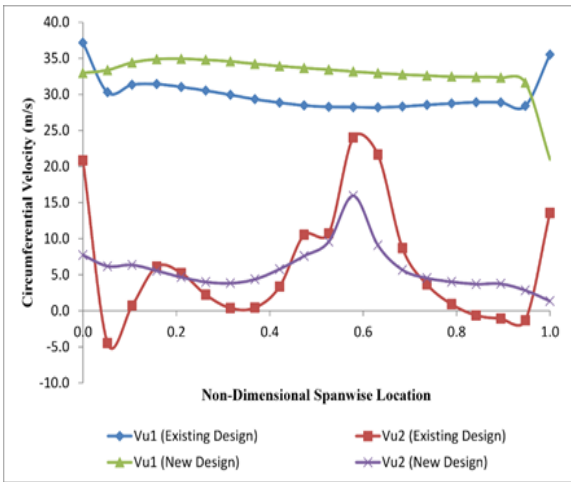

Figure 14. Circumferential velocity distribution at the inlet (V_{u1}) and outlet (V_{u2}) of the runner for the existing and new designs.

Table 5. Runner optimization through several CFD aided designs.

Version	Changed Parameter	Optimization Results	Runner Efficiency (%)	Head in-out (m)	Power (MW)
V01	Beta distribution of the original runner is smoothed. NACA 0040 profile is used.	Rise in head and flow rate.	95.0	140.3	8.01
V02	Blade is turned into an X shape with defining 1^0 to 5^0 lean angle from leading edge	Improvement in pressure distribution.	96.1	143.6	8.27
V03	Blade length is shortened 2 cm. Leading and trailing edge are thickened 1 mm.	Decreasing the blade length decreased the friction losses. Rise in power.	96.2	144.3	8.32
V04	Blade length is shortened 2cm more. Leading and trailing edges are thickened 2 mm.	Decreasing the blade length decreased friction losses. Rise in power. Cavitation characteristics worsen.	96.3	145.6	8.4
V05	Leading edge beta values are settled to 30^0 (from V3)	Leading edge separations disappeared. Travelling bubble cavitation is observed. Power decreased.	95.6	143.6	8.23
V06	Meridional profile is tightened by decreasing the beta angles from hub and shroud layers 3^0 to 7^0.	Power and efficiency increased. Velocity vectors are improved.	96.0	143.4	8.24
V07	Blade theta distribution is linearized.	Improvement in cavitation characteristics, drop in performance.	95.2	140.6	8
V08	Trailing edge beta angles are changed between 11^0-19^0 (from V6)	Improvement in power and efficiency; however, no important change in cavitation characteristics, separations are seen.	96.8	142.6	8.26
V09	Leading edge beta angles are increased 5^0 for all layers	Leading edge cavitation. No important change in performance	96.8	142.5	8.26
V10	Stronger X-Blade design	For several layers, separations disappear. Efficiency increases. (From V 6)	96.4	143.2	8.26
V11	Meridional profile is widened by decreasing the beta angles from hub and shroud 10^0.	Power and efficiency drop	95.3	141.8	8.1
V12	The change is made on V8. Blade trailing edge beta values are increased 3^0	Improvement in cavitation characteristics and drop in power.	96.8	140.8	8.15
V13	The change is made on V8. Blade trailing edge beta values are increased 1^0	Improvement in cavitation characteristics and drop in power.	96.8	140.7	8.16
V14	Second layer beta values are increased 2^0	More homogenous V_m and V_u distribution. The performance is similar to V11.	95.4	141.3	8.08
V15	The change is made on V12. Second layer beta values are increased 5^0	Separations increased, drop in head and power.	96.1	138.6	7.98
V16	The change is made on V13. Leading edge beta values are decreased and linear distribution is ensured	Separations substantially decrease. Performance is improved.	96.8	141.6	8.21
V17	Guide vane angle is settled to 16.3^0 (From V16)	Stagnation point is at the blade tip, drop in power, separations reappear.	96.7	140.9	8.16
V18	Blade thickness profile is turned to a NACA profile	Better cavitation characteristics, efficiency decreases.	96.4	140.8	8.13
V19	10^0 leaning is defined from shroud layer in the rotation direction	Better cavitation characteristics and drop in power.	96.5	140.5	8.12
V20	5^0 leaning is defined from shroud layer in the rotation direction (Based on V16)	Better cavitation characteristics and no change in power.	96.6	140.1	8.11
V21	5^0 leaning is defined from shroud layer in the reverse of the rotation direction (Based on V16)	Power rises and adverse impact on cavitation characteristics	96.3	142.6	8.22
V22	10^0 leaning is defined from shroud layer in the reverse of the rotation direction (Based on V16)	Power rises and adverse impact on cavitation characteristics	95.5	144.2	8.25
V23	Leading edge beta values are decreased 2^0 for central layer (Based on V19)	Uniform velocity distribution. Head losses are decreased.	96.0	143.5	8.25
V24	Leading edge beta values are decreased 4^0 for central layer (Based on V23)	Cavitation characteristics get worse.	95.8	145.0	8.33
V25	Beta values are decreased 6^0 for middle layer. (Based on V23)	Non-uniform pressure distribution.	96.6	144.7	8.36
V26	Guide vane angle is changed to 16^0. (Based on V23)	Better velocity distribution and cavitation properties.	96.8	144.6	8.38
V27-V40	Leading edge beta angles settled to their optimum values	Required performance is obtained with no separation phenomena	96.9	143.9	8.33

Full turbine analyses are performed and power versus efficiency graph is obtained for different guide vane angles. The modification of guide vane and efficiency brings 3% efficiency gain to the system on average. Fig. 15 shows the efficiency versus power values for a head of 167 m as a representative graph for the efficiency gain.

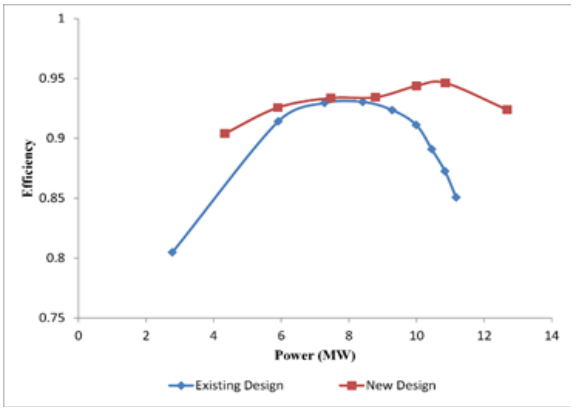

Figure 15. KEPEZ-I efficiency gain with new runner and guide vane design (for 167 m head)

Fig. 16 shows that static pressure decreases from the leading edge to the trailing edge on both suction and pressure sides. The pressure difference between these two sides generates angular momentum and it imparts a rotational motion to the turbine. Suction side trailing edge has the lowest pressure values which can lead to cavitation damage at the runner. In the existing design, there is an insufficient pressure distribution on the suction side of the blade especially close to the shroud, which causes trailing edge cavitation.

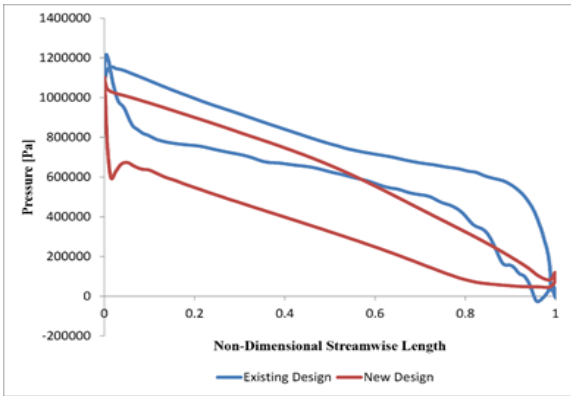

Figure 16. Blade loading for the existing and new designs (80% span)

Full turbine analyses are carried out for different heads and guide vane openings with new guide vane and runner design. A hill chart is generated as shown in Fig. 17. Head range of the turbine is changed between 141 m to 167 m and guide vane opening is changed from 15^0 to 30^0. 40 full turbine analyses are conducted to observe the behavior of the turbine for different flow rate and head combinations. When pure hydraulic efficiency without leakage and disk

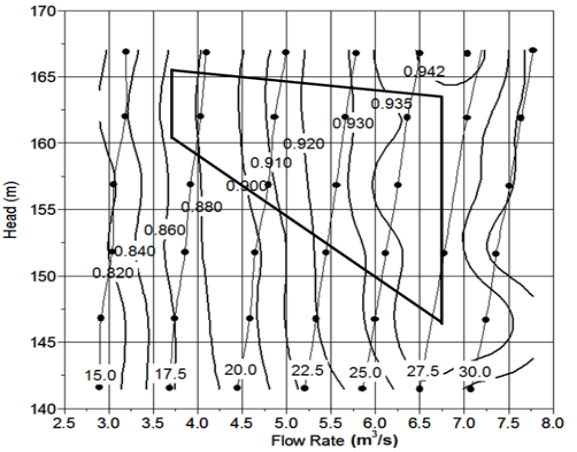

Figure 17. Hill chart for the new design

friction and losses is taken into consideration, maximum efficiency value reaches 94.54%.

Cavitation damage is an important problem in the existing design. New design prevents cavitation damage. Figure 18 shows pressure distribution for the newly designed blade. The pressures are higher than the vapor pressure. Fig. 19 shows the vapor volume fraction isosurfaces. As seen in the figure, there is no vapor on the runner surface.

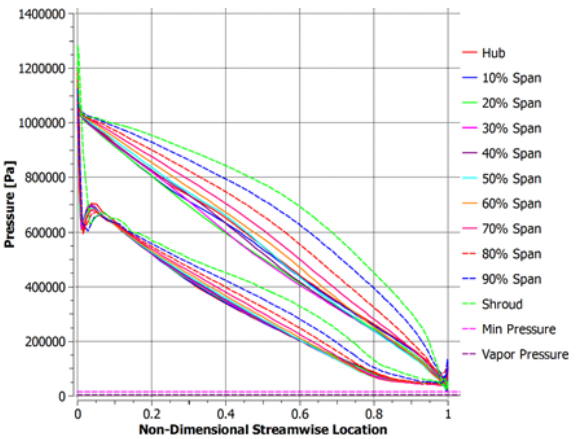

Figure 18. Pressure distribution on the new runner blade at the design condition

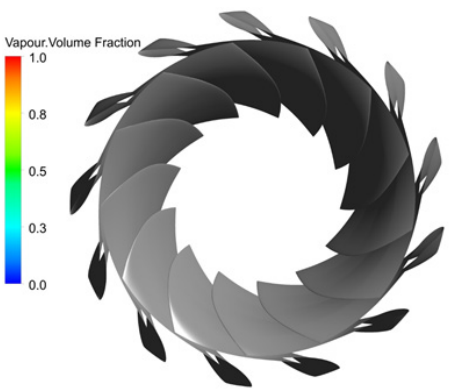

Figure 19. Vapor volume fraction isosurfaces on the new runner blades at the design condition

Structural analysis of the new runner and guide vane designs

The structural analyses of the guide vanes and the runner are performed using Ansys software based on Finite Element Method (FEM). Pressure distribution on the blade surface is used as input for the structural analyses. The runner blade surface is divided into eight different regions and overall pressure is identified for each region based on the blade loading. High pressure region refers to the pressure side and low pressure region refers to the suction side of the runner blade. Fixed support is used for the runner-shaft connection region. The material is selected as X3CrNiMo 13-4 (1.4313) stainless steel for the runner. The gravitational acceleration is also used in the simulations. Tensile strength of the material is 700 MPa. The results are evaluated based on the von-Mises and shear stresses. It is checked whether these stresses are below the tensile strength for structural safety. Fig. 20 shows the von Mises and shear stresses for the runner. As seen from the figure, the maximum von-Mises stress is computed to be 267 MPa. This maximum occurs on the shroud and the trailing edge. The safety factor is calculated to be 2.6 per the most critical point which shows that the blade is safe for operation. The maximum of the shear stress is 142 MPa at the same point, which is also in the safe zone.

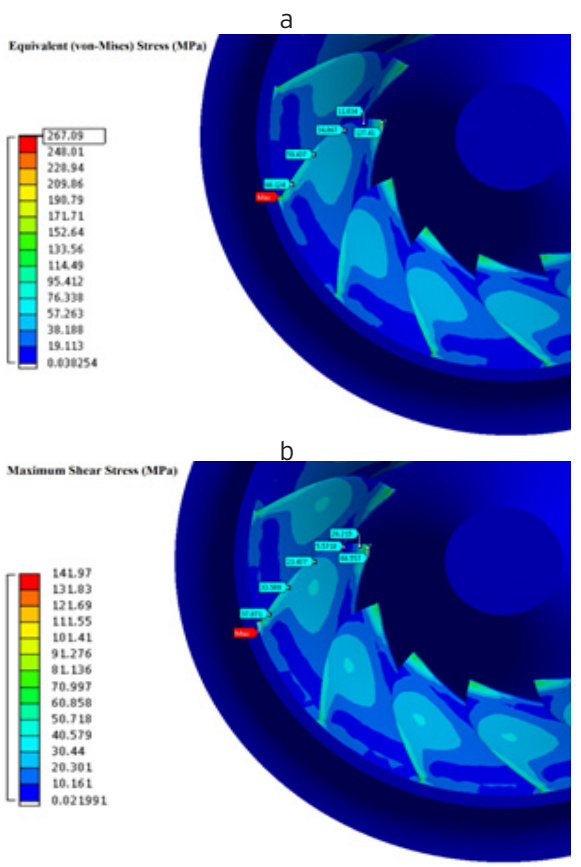

Figure 20. Stress distribution on the new runner blade, a. Von Misses stresses, b. Shear stresses

Structural analysis of the guide vane is performed using the same methodology as the runner blade. Maximum von Misses and shear stresses are computed as 278 and 157 MPa, respectively. Fig. 21 shows the stress distribution on the guide vanes. The safety factor is calculated to be 2.5 for the critical point. It is observed that the guide vane geometry is safe for operation, as well.

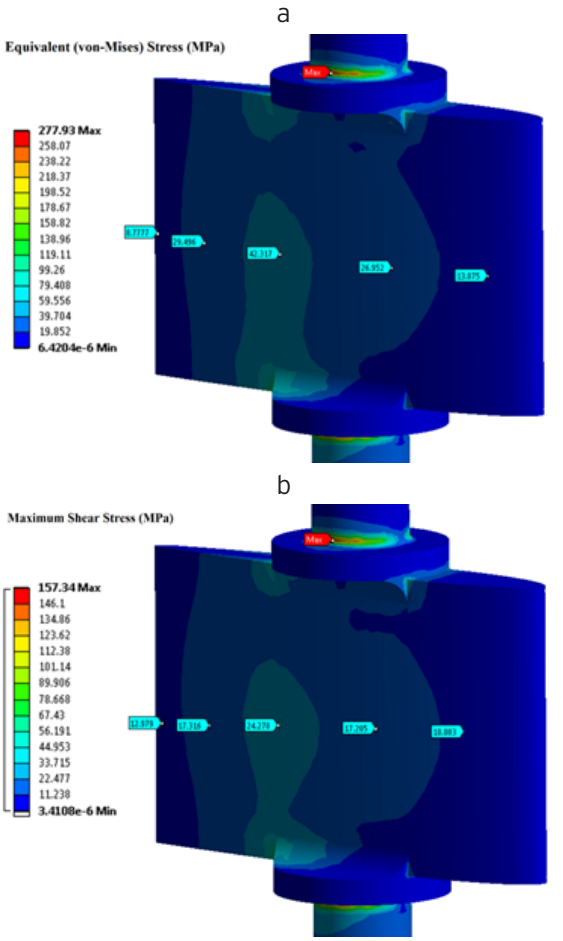

Figure 21. Stress distribution on the new guide vanes, a. Von Misses stresses, b. Shear stresses

CONCLUSION

CFD allows improvements in design. Robust, economic and efficient design can be achieved with the usage of computational techniques. Full turbine and part by part simulations of an existing turbine are performed. The design is improved with the help of computational techniques, by redesigning the guide vanes and runner of the turbine which are the only parts that are not actually buried.

The new design provides an increase in power and efficiency for the design point, as well as better cavitation characteristics. The general points of this specific rehabilitation study that can be applicable for all Francis turbine rehabili-

tation processes can be summarized as:

(1) Not only the technical drawings, but also the laser scanning measurements for the turbine components that will not be changed in the rehabilitation process are necessary for turbine design, since some of the parts may be different than the technical drawings because of time dependent wear of the material.

(2) Using X shaped blade runners instead of traditional runner geometries, improves the cavitation characteristics of the turbine and it contributes to efficiency and power rise.

(3) If there is a negative pressure zone which causes a reduction in the generated power and efficiency, introducing a lean from the hub in the direction of rotation can result in an increase in performance.

(4) To compare the conventional and the new state of the art CFD aided design, the best way is to generate a hill chart using the simulation results for many operating points including the design point, as with a hill chart, not only operating point but also operating region and part load behaviors of the turbine can be investigated.

The work is limited to steady-state simulations since full turbine analyses are performed for both design and off-design conditions. The next step in terms of the computational study is to perform unsteady simulations to observe the time dependent nature of the flow if there is. The next step in this research is to manufacture a model and perform model tests of the designed turbine based on IEC 60193 standards.

ACKNOWLEDGEMENTS

This work is financially supported by Tübitak Kamag under grant number 113G109. The computations are performed at TOBB ETU Hydro Energy Research Laboratory (ETU Hydro) financially supported by Turkish Ministry of Development.

REFERENCES

[1] Choi HJ, Zullah MA, Roh HW, Oh SY, Lee YH. CFD validation of performance improvement of 500 kW Francis turbine. Renewable Energy, 54 (2013) 111–123.

[2] Beatove SL, Ruiz GM, Arboleda, BQ, Bustamante OS. CFD: Numerical simulations of Francis turbines. Rev. Fac. Ing Univ. Antioquia, 51 (2010) 31–40.

[3] Qian ZD, Yang J.D, Huai WX. Numerical simulation and analysis of pressure pulsation in Francis hydraulic turbine with air admission. Journal of Hydrodynamics, Ser. B 19 (2007) 467–472.

[4] Su WT, Li FC, Li BX, Wei XZ, Zhao Y. Assessment of LES performance in simulating complex 3D flows in turbo–machines. Engineering Applications of Computational Fluid Mechanics, 6(3) (2012) 356–365.

[5] Patel K, Desai J, Chauhan V, Charnia S. Development of Francis turbine using Computational Fluid Dynamics. 11st Asian International Conference on Fluid Machinery and 3rd Fluid Power Technology Exhibition, 2011.

[6] Kaniecki M, Lojek A, Hajdarowicz M. Rehabilitation of medium–head hydropower plants with exploited Twin–Francis Turbines, Congress SHP, 2014.

[7] Akin H, Aytac Z, Ayancik F, Ozkaya E, Arioz E, Celebioglu K, Aradag, S. A CFD aided hydraulic turbine design methodology applied to Francis turbines. IEEE 4th International Conference on Power Engineering, Energy and Electrical Drives (POWERENG), 2013.

[8] Gohil PP, Saini RP. CFD: Numerical analysis and performance prediction in Francis turbine. IEEE 1st International Conference on Non–Conventional Energy (ICONCE), 2014.

[9] Shukla MK, Jain R, Prasad V, Shujla SN. CFD Analysis of 3–D Flow for Francis Turbine, MIT International Journal of Mechanical Engineering, 1 (2011) 93–100.

[10] Bornard L, Debeissat F, Labrecque Y, Sabourin M, Tomas L. Turbine hydraulic assessment on optimization in rehabilitation projects. IOP conference series: Earth and Enviromental Science, 22 (2014).

[11] Xi–de L, Yuan H. Numerical simulation–driven hydrodynamic optimization for rehabilitation and upgrading of hydro turbines. Power and Energy Engineering Conference, Asia–Pacific, 2009.

[12] Michel B, Kunz T. Rehabilitation of hydro generating units. Power Russia Conference, Moscow, Russia, 2006.

[13] Sepetci, G, Cetinturk H, Ozkan SY, Yuksel O, Karadeniz C, Celebioglu K, Tascioglu Y, Aradag S. Conceptual design of a hydroelectric power plant for a rehabilitation project. HEFAT 2016 conference, Malaga, Spain, 2016.

[14] Ansys CFX Users's Manual v16, 2016.

[15] Keck H, Sick M. Thirty years of numerical flow simulation of Francis Turbines. Rev. Fac. Ing. Univ. Antioquia, 51 (2010) 34–33.

[16] Lenarcic M, Eichhorn M, Schoder SJ, Bauer C. Numerical investigation of a high head Francis turbine under steady operating conditions using foam–extend, Journal of Physics: Conference Series, 2015.

[17] Tonello N, Eude Y, Meux BL, Ferrand M. Frozen Rotor and Sliding Mesh Models Applied to the 3D Simulation of the Francis–99 Tokke Turbine with Code_Saturne, IOP Conf. Series: Journal of Physics: Conf. Series, 2017.

[18] Laouari A, Ghenaiet A. Simulations of Steady Cavitating Flow in a Small Francis Turbine, International Journal of Rotating Machinery, 2016.

[19] Kapoor H. Open Source Mesh Generation and CFD Simulations for Francis Turbine. MSc Thesis, Chalmers University of Technology, Sweden, 2014.

[20] Ayli E, Celebioglu K, Aradag S. Determination and generalization of the effects of design parameters on Francis turbine runner performance. Engineering Applications of Computational Fluid Mechanics, 10 (1) (2016) 547–566.

[21] Ayli E, Kaplan A, Cetinturk H, Kavurmaci B, Demirel G, Celebioglu K, Aradag S. CFD analysis of 3D flow for 1.4 MW Francis turbine and model turbine manufacturing. 35th Computers and Information in Engineering Conference, Boston, MA, USA, 2015.

[22] Michel B, Couston M, Francois M. Hydro turbines rehabilitationperformance. Engineering Applications of

Computational Fluid Mechanics, 10 (1) (2016) 547–566.
[23] Billda, J T, Holt BG. Three Gorges Project: Review of GE Energy Norwy's hydraulic design. Symposium on Hydraulic Machinery and Systems, 20th IAHR Symposium, Charlotte, NC, USA, 2010.
[24] Brekke H. Design, performance and maintenance of Francis turbines. Global Journal of Researches in Engineering, Mechanical and Mechanics Engineering, 13 (5) (2013).
[25] Krivchenko GI. Hydraulic machines: turbines and pumps. Boca Raton, FL: Lewis publishers, 1994.